Nomenclature

T_i	i-th turbine
$P_{av,i}$	Available power for i-th turbine
$P_{r,i}$	Reference power for i-th turbine
$P_{w,i}$	Generated power for i-th turbine
$P^p_{av,i}$	Available power for i-th subset
$P^p_{r,i}$	Reference power for i-th subset
$P^p_{w,i}$	Generated power for i-th subset
$P_{w,tot}$	Total generated power
$P_{av,tot}$	Total available power
P_{dem}	Power demanded by TSO
P_{res}	Power reserve ($P_{\text{res}} = P_{\text{av,tot}} - P_{\text{w,tot}}$)
v_∞	Free-stream wind speed
φ	Free-stream wind speed direction
m	Number of subsets
$\mathscr{K}$	Set of indexes in the subset $\mathscr{K} = \{1, \ldots, m\}$
$\mathscr{P}_l$	l-th partition
$\mathscr{P}^*$	Partition set
$\overline{\mathscr{V}}_{so}$	Set of source elements
$\overline{\mathscr{V}}_{in}$	Set of sink elements
τ_i	Network resource-feeding indeces
$\mathbb{R}$	Set of real numbers
$\mathbb{N}$	Set of natural numbers
$\mathbf{I}_n$	Identity matrix of dimension $n \times n$

direction method of multipliers (ADMM), dual-decompo-sition and consensus-based control algorithms have attracted more attention for wind farm control [13–16]. In Ref. [13], fast gradient methods via dual-decomposition are used for power regulation and load alleviation, in which most of the computational tasks are shared by local distributed predictive controllers at wind turbine level and reducing the computational cost of the central unit. ADMM was also used in Ref. [10] to solve iteratively a clustering-based distributed optimization problem in order to improve yaw misalignment issues of turbines within wind farms and the total power production. Other limited-communication methodologies use consensus algorithms to maximize the power generation and stored kinetic energy [17,18]. These consensus algorithms have been successfully used for optimal power-sharing between wind farms and energy storage devices [16,19]. Non-centralized control approaches have also been used in wind farms to mitigate negative wake effects in the power production by computing axial induction factors or yaw misalignment [11,15]. As these approaches rely on complex wake models and complex non-convex optimization problems, the online implementation might be difficult.

Extending the previous results in Ref. [20], the present paper proposes a hierarchical non-centralized model predictive control (MPC) scheme relaying on a virtual partitioning of a large-scale wind farm. The main contributions are:

- Improvement of the partitioning procedure by casting it as a mixed-integer linear optimization problem taking into account the coupling among turbines caused by wakes.
- Design of a three-level MPC scheme aimed to ensure the power regulation imposed by the TSO and seeking to maximize the power reserve available for ancillary service provision. With the wind farm divided into a few almost uncoupled subsets, the wind farm control is stated using a non-centralized scheme in order to reduce computational burden and high information exchange and thus to increasing the system resiliency.
- The evaluation through numerical simulations of the proposed control scheme in a full-scaled wind farm of 42 turbines using SimWindFarm [21].

The remainder of the paper is organized as follows: Section 2 introduces the wind turbine power generation and wake effect. Section 3 presents the optimal partitioning algorithm aimed to divide the wind farm into almost uncoupled smaller parts and the optimal number of turbines per subset. The non-centralized predictive control architecture is designed in Section 4. In Section 5, the proposed partitioning and control schemes are evaluated in a farm of 42 wind turbines using a wind farm simulator including wake interaction among the turbines. Finally, conclusions and future lines are presented in Section 6.

2. Wind power and wake effect

Considering a wind farm with n turbines, the power generated by the i-th turbine T_i is given by

$$P_{w,i} = \frac{\rho \pi R^2}{2} C_p(a_i) v_i^3, \tag{1}$$

where ρ is the air density, R is the rotor radius, v_i indicates the incoming wind speed and C_p is the power coefficient that depends on the induction factor a_i, [22].

The wind speed faced and thus the power produced by turbine T_i depend on the free-stream wind speed v_∞ and the generation conditions of neighbour turbines. A wind turbine disturbs the air flow producing wakes that expand in the outflow field affecting the speed faced by the downstream turbines.

Several wake models have been proposed in the literature to estimate the wake effect on the wind speed v_i, the most commonly used being the *Park model* [23]. This model estimates the effect of multiple wake interactions assuming that wakes expand as a cone-like fashion with circular cross section for a given free-stream wind speed v_∞, and the wind speed profile has a top-hat shape in the crosswind direction. Under these assumptions, the wind speed faced by the i-th turbine $\mathbf{T}_i$ is computed as

$$v_i = v_\infty \left(1 - 2\sqrt{\sum_{j \in \mathscr{N}_i} \left(2(1-a_j)\frac{R}{r_{ij}(x_{ij})}\right)^2 \frac{A^s_{ij}(x_{ij})}{A_{0,i}}}\right), \tag{2}$$

where x_{ij} is the distance in the x-direction between turbines $\mathbf{T}_j$ and $\mathbf{T}_i$, $r_{ij}(x_{ij}) = R + z_0\, x_{ij}$ is the radius of the wake generated by turbine $\mathbf{T}_j$, z_0 the roughness coefficient and $\mathscr{N}_i$ is the set of indeces corresponding to the turbines upstream of $\mathbf{T}_i$. The symbols $A_{0,i}$ and $A^s_{ij}(x_{ij})$ denote the rotor area and the shadowed area due to the upstream turbine, respectively (see Fig. 1). If the wind turbines have the same radius R, then the shadowed area can be computed as

$$A^s_{ij}(x_{ij}) = r_{ij}(x_{ij})^2 \cos^{-1}\left(\frac{L_{ij}}{r_{ij}(x_{ij})}\right) + \cos^{-1}\left(\frac{d_{ij} - L_{ij}}{r_{ij}(x_{ij})}\right) + d_{ij} z_{ij}, \tag{3}$$

with L_{ij} the distance between the centres of the wake area A^x_{ij} and the shadowed area A^s_{ij}, d_{ij} the distance between the centres of the wake area A^x_{ij} and the rotor area $A_{0,i}$, and z_{ij} the vertical distance between the intersection points of the previously mentioned areas

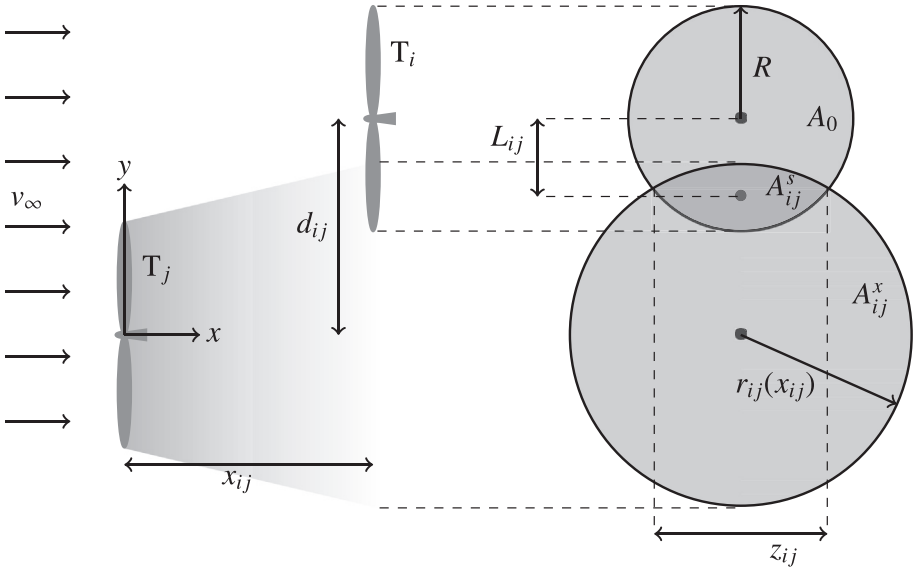

Fig. 1. Representation of the wake effect caused by turbine $\mathbf{T}_j$ over turbine $\mathbf{T}_i$.

(see Fig. 1).

The wake impact on the wind speed faced by downstream turbines depends on the free-stream wind speed direction φ (defined as the angle between v_∞ and the farm layout as indicated in Fig. 4) and the turbine geographical disposition within the farm [24]. Hence, the wake effect faced by some turbines can be either partial or total as shown in Fig. 1. As stated before, the effect over downstream turbines also depends on the operational conditions of upstream turbines, which are taken into account with the induction factor in (2). Nevertheless, the degree of coupling due to wake effects between turbine $\mathbf{T}_i$ and $\mathbf{T}_j$ is basically a function of the wind speed direction and wind farm layout (location and distance among turbines).

In large wind farms, couplings among turbines caused by wakes are significant and lead to substantial power losses. Such negative impact can be reduced with suitable control strategies that send power commands to each turbine considering couplings. In this circumstance, centralized control approaches may demand large information sharing between turbines and the central controller. Complex communications and large information exchange result difficult to process over times suitable to satisfy the grid requirements (typically about seconds [25]) and the high communication dependency make the system exposed to failures. For this reason, in this work, a possible solution to mitigate the aforementioned issues is proposed by designing a non-centralized wind farm control strategy. In this approach, turbines are sorted into subsets controlled by independent local controllers, which are local decision makers that use only the portion of information corresponding to the specific subset of turbines.

3. Wind farm partitioning

As the first step towards optimally designing a non-centralized control strategy, the wind farm is partitioned into several almost uncoupled subsets of turbines. That is, wind turbines are organized in subsets according to the coupling level associated with the wake effect. Among the different approaches proposed for partitioning large-scale systems [8,14,26], here the partitioning approach proposed in Ref. [20] is considered and improved in order to provide a more robust partitioning algorithm.

3.1. Partitioning problem

With the aim of considering wake effects, the interactions due to the wake propagations are represented as a weighted directed graph $\mathcal{G} = (\mathcal{V}, \mathcal{E})$, where $\mathcal{V} = \{1, 2, \ldots, n\}$ is the set of vertices, where each vertex corresponds to a wind turbine and $\mathcal{E} = \{(i,j) : i,j \in \mathcal{V}\}$ is the set of edges with weights

$$\varepsilon_{ij} = \left| \frac{R}{r_{ij}(x_{ij})} \right| \frac{A^s_{ij}(x_{ij})}{A_0}, \tag{4}$$

if turbine $\mathbf{T}_i$ is placed downstream of turbine $\mathbf{T}_j$ (i.e., the wind speed faced by the i-th turbine is affected by the wake caused by j-th turbine); otherwise, $\varepsilon_{ij} = 0$ [14].

Then, according to the wind farm layout and the predominant free-stream wind speed direction φ, the wind farm can be sorted in m subsets and the number of turbines within each subset can be found by solving the following optimization problem:

$$\underset{\delta_{il}}{\textbf{minimize}} \delta_{il} \sum_{q=1}^{3} w_q f_q(\delta_{il}), \tag{5a}$$

$$\textbf{subject to} \sum_{i \in \mathcal{V}} \delta_{il} \geq 1, \quad \forall\, l \in \mathcal{K} \tag{5b}$$

$$\sum_{l \in \mathcal{K}} \delta_{il} = 1, \quad \forall\, i \in \mathcal{V}, \tag{5c}$$

with $\delta_{il} \in \{0, 1\}$ a Boolean decision variable such that $\delta_{il} = 1$ if turbine $\mathbf{T}_i$ belongs to subset l, with $l \in \mathcal{K} = \{1, 2, \ldots, m\}$, and 0 otherwise. The non-empty constraint (5b) and the exclusive constraint (5c) ensure that the subsets cannot be empty and turbine $\mathbf{T}_i$ can only belong to one subset l.

The objective function (5a) consists of three terms weighted by $w_q > 0$ $(q = 1, 2, 3)$:

1. The first term f_1 in the objective function (5a) is stated as the sum of the edge weights at each partition $l \in \mathcal{K}$, i.e.,

$$f_1 \triangleq -\sum_{l\in\mathscr{K}}\sum_{i\in\mathscr{V}}\sum_{j\in\mathscr{V}\setminus\{i\}}(\varepsilon_{ij}+\varepsilon_{ji})\delta_{il}\delta_{jl}. \tag{6}$$

Depending on farm layout and the v_∞ direction, only a number of downstream turbines is affected by the wake caused by an upstream turbine. The aim of this term is to consider the wake interactions among the turbines, such that the coupling levels among turbines in the same partition is maximized in order to ensure that turbines coupled by the same wake belong to the same subset.

2. The second term is added to (5a) in order to minimize the distance d_{ij} between turbines belonging to the same subsets, i.e.,

$$f_2 \triangleq \sum_{l\in\mathscr{K}}\sum_{i\in\mathscr{V}}\sum_{j\in\mathscr{V}\setminus\{i\}} d_{ij}\delta_{il}\delta_{jl}. \tag{7}$$

There might be cases where there is no coupling among turbines, i.e., $\sum_{i\in\mathscr{V}}\sum_{j\in\mathscr{V}\setminus\{i\}}(\varepsilon_{ij}+\varepsilon_{ji})=0$, e.g., when wind turbines are located in a row (or a column) and the freestream wind direction is such that the wakes generated by the upstream turbines do not affect any other turbine. In such a case, to guarantee a unique solution, turbines can be arranged according to their proximity.

3. Finally, in order to balance the number of turbines in each subset, an extra term is added to minimize the difference between the number of turbines among all subsets, i.e.,

$$f_3 \triangleq \sum_{l=1}^{m-1}\sum_{l'=l+1}^{m}\left|\sum_{i\in\mathscr{V}}\delta_{il}-\sum_{j\in\mathscr{V}}\delta_{jl'}\right|. \tag{8}$$

Avoiding significant differences between the number of nodes in the subsets will balance the computational burden of finding the optimal solution for each subset.

Setting the weights w_q, the aforementioned objectives are hierarchically prioritized to find the optimal partition $\mathcal{P}^* = \{\mathcal{P}_1,\ldots,\mathcal{P}_m\}$.

The optimization problem (5) is nonlinear; however it can be recast as a mixed-integer linear programming problem as follows. The procedure to transform products of logical variables, in terms of linear inequalities was presented in Ref. [27], which however requires the introduction of auxiliary Boolean variable δ_{ijl} such that $\delta_{ijl}\triangleq\delta_{il}\delta_{jl}$. Notice that $\delta_{ijl}=1$ if and only if $\delta_{il}=1$ and $\delta_{jl}=1$, and therefore

$$\delta_{ijl}=\begin{cases}-\delta_{il}+\delta_{ijl}\le 0,\\ -\delta_{jl}+\delta_{ijl}\le 0,\\ \delta_{il}+\delta_{jl}-\delta_{ijl}\le 1.\end{cases}$$

Let us also define a dummy variable $\varrho_{ll'}\in\mathbb{R}$ such that $\varrho_{ll'}\ge\left|\sum_{i\in\mathscr{V}}\delta_{il}-\sum_{i\in\mathscr{V}}\delta_{jl'}\right|$, then (8) can be replaced by

$$f_3=\sum_{l=1}^{m-1}\sum_{l'=l+1}^{m}\varrho_{ll'}. \tag{9}$$

Therefore, the optimization problem (5) becomes

$$\underset{\delta_{ijl},\varrho_{ll'}}{\textbf{minimize}}.\ \sum_{q=1}^{3}w_q f_q\left(\delta_{ijl},\varrho_{ll'}\right), \tag{10a}$$

$$\textit{subject to}\sum_{i\in\mathscr{V}}\sum_{j\in\mathscr{V}\setminus\{i\}}\delta_{ijl}\ge 1,\quad \forall\ l\in\mathscr{K}, \tag{10b}$$

$$\sum_{l\in\mathscr{K}}\delta_{ijl}=1,\quad \forall\ i,j\in\mathscr{V}, \tag{10c}$$

$$-\delta_{il}+\delta_{ijl}\le 0,\quad \forall\ i,j\in\mathscr{V},\ \forall\ l\in\mathscr{K}, \tag{10d}$$

$$-\delta_{jl}+\delta_{ijl}\le 0,\quad \forall\ i,j\in\mathscr{V},\ \forall\ l\in\mathscr{K}, \tag{10e}$$

$$\delta_{il}+\delta_{jl}-\delta_{ijl}\le 1,\quad \forall\ i,j\in\mathscr{V},\ \forall\ l\in\mathscr{K}, \tag{10f}$$

$$\sum_{i\in\mathscr{V}}\delta_{il}-\sum_{j\in\mathscr{V}}\delta_{jl'}\le\varrho_{ll'},\quad 1\le l\le m-1, \tag{10g}$$

$$\sum_{i\in\mathscr{V}}\delta_{il}-\sum_{j\in\mathscr{V}}\delta_{jl'}\ge-\varrho_{ll'},\quad 1\le l\le m-1, \tag{10h}$$

where $l'=l+1$ and f_q $(q=1,2,3)$ are given in (6), (7) and (9). As a consequence of using the auxiliary Boolean variable δ_{ijl}, constraints (10d)-(10f) must be added to the original problem (5) [27], and the original no-empty and exclusive constraints in (5b) and (5c) must be rewritten as (10b) and (10c), respectively. Additional constraints (10g) and (10h) are needed to be able to use the dummy variable $\varrho_{ll'}$ and hence using (9) instead of (8).

3.2. Number of subsets

In order to solve the m-partitioning problem (10), it is necessary to provide the number of subsets m. A detailed strategy to determine this number for a drinking water network is proposed in Ref. [26]. In the current work, a similar approach is presented assuming that the air flow within a wind farm can be modeled as a simplified flow-based distribution network. Many engineering systems have been modeled as flow-based distribution systems [9,26], which consist of several elements of diverse nature, e.g., storage, actuator, joint, sink, source and flow. Unlike other energy sources, wind cannot be stored, and hence the wind flow in a farm can be obtained identifying only the following elements:

1. *Source:* element generating the resource. It is equivalent to the turbine facing the free-stream wind condition v_∞ and generating the wake in the outflow field. The set of these elements is denoted by $\overline{\mathscr{V}}_{\mathbf{so}}$.
2. *Actuator:* element that receives and provides the resources. The set of actuator elements is denoted by $\overline{\mathscr{V}}_{\mathbf{ac}}$ and corresponds to the set of turbines increasing the wake effect generated by the upstream turbines $j\in\overline{\mathscr{V}}_{\mathbf{so}}$ proportionally to the operational conditions and, in turn, affected by the wakes generated by the upstream turbines.
3. *Sink:* element that receives the resource from either the source and/or the actuator. It is equivalent to the turbine only receiving wakes, e.g., the most downstream turbine. The set of sinks is denoted by $\overline{\mathscr{V}}_{\mathbf{si}}$.
4. *Link:* directed link (i,j) allowing resource flow from an element i to j. For a wind farm, this link corresponds to the wake generated by the turbine $i\in\overline{\mathscr{V}}_{\mathbf{so}}\cup\overline{\mathscr{V}}_{\mathbf{ac}}$ and moving through a turbine $j\in\overline{\mathscr{V}}_{\mathbf{ac}}\cup\overline{\mathscr{V}}_{\mathbf{si}}$. The set of link elements is denoted by $\overline{\mathscr{E}}\subset\{(i,j):i,j\in\overline{\mathscr{V}}\}$, with $\overline{\mathscr{V}}=\overline{\mathscr{V}}_{\mathbf{so}}\cup\overline{\mathscr{V}}_{\mathbf{si}}\cup\overline{\mathscr{V}}_{\mathbf{ac}}$.

Therefore, the flow-based distribution system can be identified as a directed graph $\overline{\mathscr{G}}=(\overline{\mathscr{V}},\overline{\mathscr{E}})$ where each element $i\in\overline{\mathscr{V}}$ has a direct relationship with the turbines in the graph $\mathscr{G}$. The introduced elements for a flow-based distribution system and the representation of the system by a directed graph allow finding the

number of subsets as proposed in Ref. [26], where three further indicators are defined:

1. *Network resource-feeding index*, denoted by τ_i with $i \in \overline{\mathscr{V}} \setminus \overline{\mathscr{V}}_{\mathbf{so}}$, gives information about the number of sources or actuator elements that provide the wakes for the element $i \in \overline{\mathscr{V}} \setminus \overline{\mathscr{V}}_{\mathbf{so}}$. Assuming the graph $\overline{\mathscr{G}}$ is split into m subsets, it is possible to identify the subsets of sinks $\overline{\mathscr{V}}_{\mathbf{si},l}$ and sources $\overline{\mathscr{V}}_{\mathbf{so},l}$ for each partition $l \in \overline{\mathscr{K}}, \overline{\mathscr{K}} = \{1, \ldots, m\}$, while the maximum resource-feeding index per partition is defined by $\tau_l^* = \mathbf{max}_{i \in \overline{\mathscr{V}}_{\mathbf{si},l}} \tau_i$.
2. *Sink co-relation index*: The proportion of sinks in each subset $l \in \overline{\mathscr{K}}$ with respect the total number of sinks in the flow-based graph $\overline{\mathscr{G}}$, i.e., $\sigma_l = \sum_{i \in \overline{\mathscr{V}}_{\mathbf{si},l}} \tau_i / \sum_{i \in \overline{\mathscr{V}}_{\mathbf{si}}} \tau_i$.
3. *Resource-feeding co-relation index*: The availability of sources in the subset $l \in \mathscr{K}$ feeding the sink element $i \in \overline{\mathscr{V}}_{\mathbf{si},l}$ for which $\tau_i = \tau_l^*$. It is assessed with respect to the total number of sources $j \in \overline{\mathscr{V}}_{\mathbf{so}}$ feeding the element i, i.e., $\beta_l = \sum_{j \in \overline{\mathscr{V}}_{\mathbf{so},l}} \alpha_{ij} / \sum_{j \in \overline{\mathscr{V}}_{\mathbf{so}}} \alpha_{ij}$, where $\alpha_{ij} = 1$ if the flow element $\varepsilon_{ij} = 1$ with $\varepsilon_{ij} \in \overline{\mathscr{E}}$, and 0 otherwise.

The number of subsets is assessed by setting both a desired *maximum sink co-relation index* and a *minimum resource-feeding co-relation index*, hence the subsets should satisfy $\sigma_l \leq \sigma^*$ and $\beta_l \geq \beta^*$. The parameter σ^* is set to ensure that the number of sink elements is balanced among the subsets such that there is no subset without sinks. Furthermore, identifying for each subset the maximum resource-feeding index τ_l^* and their respective sources, it is desired that each subset includes a minimum number of these sources indicated by β^*.

3.3. Algorithm and implementation aspects

Fig. 2 summarizes the partitioning approach proposed in this paper. Assuming an initial number of subsets m, the partitioning problem for the information sharing graph $\mathscr{G}$ is first solved and the optimal partition set $\mathscr{P}^*$ is found. Then, the analogy with the flow-based distribution graph $\overline{\mathscr{G}}$ is used to check whether or not the criteria for the proper number of subsets are fulfilled. An iterative loop is repeated increasing the initial number of subsets $m = m + 1$ until the aforementioned criteria for defining the number of subsets are satisfied.

The partition obtained with the previous procedure $\mathscr{P}^*$ depends on the distances x_{ij} and the wind turbine arrangement within the farms (i.e.the set of downstream and upstream turbines), which in turn depends on the free-stream wind speed direction φ. Furthermore, the computational burden to solve the proposed partitioning problem for large-scale wind farms can be high and inconsistent with the time scale related to the variation of wind direction and the sampling time used into the wind farm controller. Nevertheless, the subsets can be determined offline and one can keep a look-up table to update the subsets whenever the predominant free-stream wind speed direction changes. As the wind speed direction is sensitive to turbulence and other atmospheric and geographical conditions such as eventual obstacles surroundings, the predominant wind speed direction can be used to select the corresponding subset.

4. Wind farm control strategy

Once the system is partitioned as indicated in the previous section for a set of predominant free-stream wind speed directions

$$\mathbf{\Phi} = \{\varphi_1, \ldots, \varphi_w\},$$

there is a set $\mathscr{P}^*$ of optimal partition sets for each angle $\varphi \in \mathbf{\Phi}$. Then, for a given direction φ and the corresponding partition set

$$\mathscr{P}^* = \{\mathscr{P}_1, \ldots, \mathscr{P}_m\},$$

the proposed non-centralized hierarchical control approach is structured as indicated in Fig. 3, where $\mathscr{P}_l$ is a set of n_l indexes corresponding to the wind turbines in the subset $l \in \mathscr{K} = \{1, \ldots, m\}$. For the sake of clarity, Fig. 3 illustrates only the signal interactions in the control algorithm and does not include the electrical interconnections.

At the highest level, the Central Controller (CC) collects information regarding the generated power $P^{\mathbf{p}}_{\mathbf{w},l}$ and the available power $P^{\mathbf{p}}_{\mathbf{av},l}$ in each subset and then sends the corresponding commands

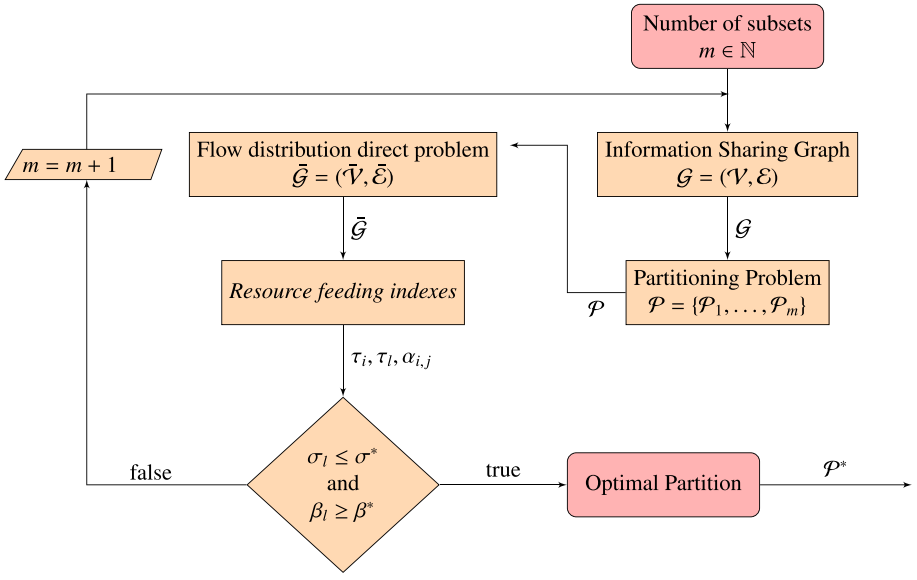

Fig. 2. Optimal partitioning algorithm flowchart.

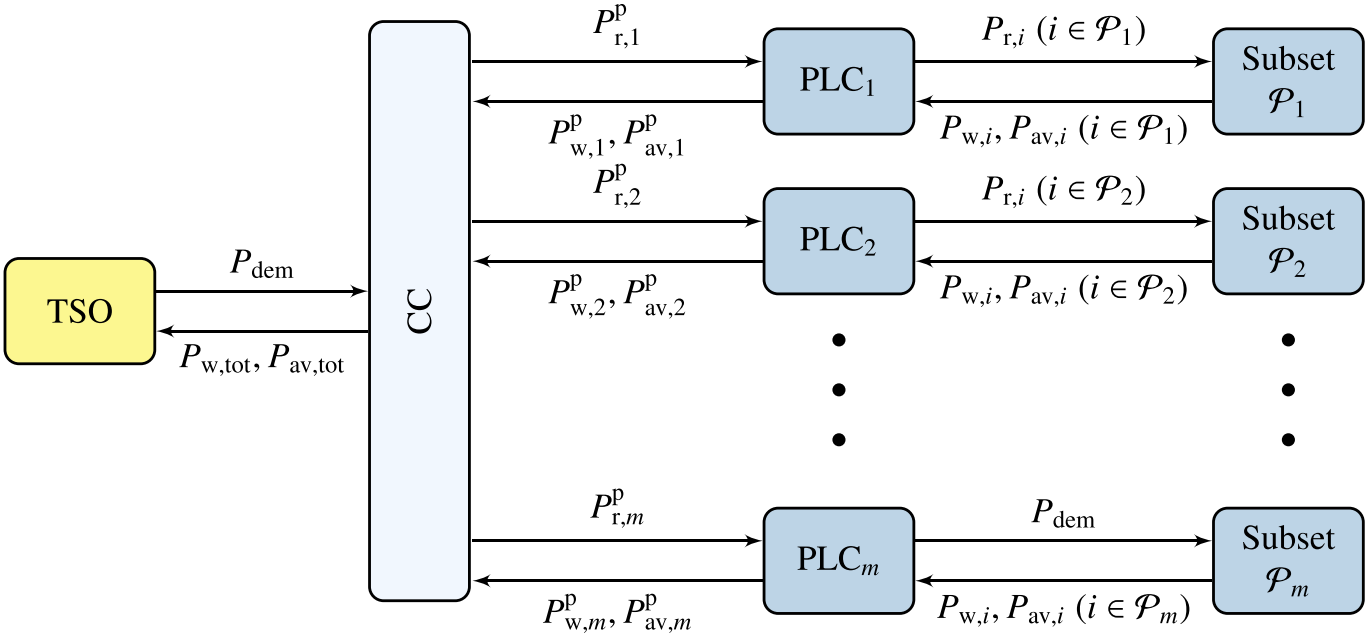

Fig. 3. Scheme of the proposed wind farm non-centralized control strategy for a given φ and the corresponding partition set $\mathscr{P}^*$ with m elements.

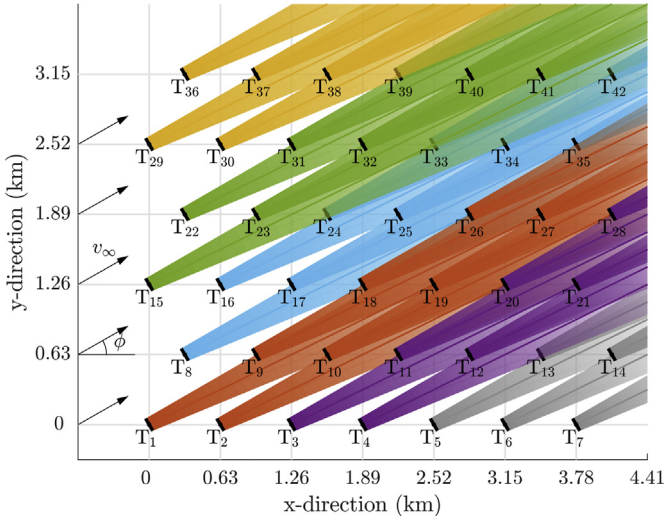

Fig. 4. Wind farm layout and optimal partitioning for a wind speed direction of $\varphi = 30^\circ$: light blue $\mathscr{P}_1$, red $\mathscr{P}_2$, green $\mathscr{P}_3$, yellow $\mathscr{P}_4$, gray $\mathscr{P}_5$, and purple $\mathscr{P}_6$. (For interpretation of the references to colour in this figure legend, the reader is referred to the Web version of this article.)

$P^{\text{p}}_{\text{r},l}$. This controller aims to ensure that the total power delivered at the Point of Common Coupling (PCC) by the wind farm $P_{\mathbf{w,tot}}$ matches the TSO's power demand $P_{\mathbf{dem}}$. In a lower level, the Partition Level Controllers (PLC) use the measure of the generated power $P_{\mathbf{w},i}$ and the available power $P_{\mathbf{av},i}$ at each turbine in the corresponding subset to impose a reference $P_{\mathbf{r},i}$ to each turbine. Finally, at the lowest level, the wind turbine control guarantees that the generated power satisfies the set-point $P_{\mathbf{r},i}$.

4.1. Wind turbine controller

Each wind turbine is equipped with a power controller that allows working in derated mode if necessary [21,22]. Thus, the power generated by the i-th wind turbine is given by

$$\dot{P}_{\mathbf{w},i} = -\frac{1}{\mu}\left(P_{\mathbf{w},i} - \mathbf{min}(P_{\mathbf{av},i}, P_{\mathbf{r},i})\right), \tag{11}$$

where μ is a time constant, $P_{\mathbf{r},i}$ is the reference sent by the PLC, and

$$P_{\mathbf{av},i} = \mathbf{min}\left(\frac{\rho\pi R^2}{2} C_{\mathbf{p,max}} v_i^3, P_{\mathbf{rated}}\right) \tag{12}$$

is the wind turbine available power, with $C_{\mathbf{p,max}} = \mathbf{max}_{a_i} C_{\mathbf{p}}(a_i)$ and $P_{\mathbf{rated}}$ the wind turbine rated power.

4.2. Partition level controllers (PLCs)

The PLCs aim to ensure the total power generated in each partition matches the power demanded by the CC. In addition, these controllers seek to distribute the power contribution of each turbine in order to maximize the total available power, which in turn maximizes the power reserve of the entire farm available for ancillary services. The power reserve is defined as $P_{\mathbf{res}} = P_{\mathbf{av,tot}} - P_{\mathbf{w,tot}}$.

For a given partition $\mathscr{P}_l$, with $l \in \mathscr{K}$ and n_l turbines, the corresponding PLC relies on an MPC strategy based on the following optimization problem:

$$\underset{\mathbf{u}_l}{\text{minimize}}\ (k) \sum_{q=1}^{3} \sum_{k=1}^{H_{\mathbf{p}}-1} \gamma_q J_q(\mathbf{x}_l(k), \mathbf{u}_l(k)) \tag{13a}$$

$$\text{subject to}\quad \mathbf{x}_l(k+j+1|k) = \mathbf{A}_{d,l}\mathbf{x}_l(k+j|k) + \mathbf{B}_{d,l}\mathbf{u}_l(k+j|k) \tag{13b}$$

$$P_{\mathbf{min}} \le u_{l,i}(k+j) \le P_{\mathbf{av},i},\ \ \forall\ i \in \mathscr{P}_l \tag{13c}$$

where $\gamma_q > 0$ are prioritization weights such that $\sum_{q=1}^{3} \gamma_q = 1$, $\mathbf{x}_l \in \mathbb{R}^{n_l}$ is the state vector and $\mathbf{u}_l \in \mathbb{R}^{n_l}$ is the vector of manipulated variables, with elements $x_{l,i} = P_{\mathbf{w},i}$ and $u_{l,i} = P_{\mathbf{r},i}$ $(i \in \mathscr{P}_l)$,

respectively. The time indices $k \in \mathbb{N}$, $j \in \{0, \ldots, H_{\mathbf{p}} - 1\}$ and the prediction horizon $H_{\mathbf{p}}$ are defined such that $\mathbf{x}_l(k+j|k)$ denotes the vector of measured generated power at the instant k corresponding to the control input $\mathbf{u}_l(k+j|k)$.

The solution of problem (13) is the optimal control input $\widehat{\mathbf{u}}_l \triangleq \widehat{\mathbf{u}}_l(k|k)$ corresponding to the set-points for each the turbine $i \in \mathscr{P}_l$. Notice that the first constraint (13b) corresponds to the discretized version of (11), used to predict the power response of the wind turbines in the partition $\mathscr{P}_l$, where $\mathbf{A}_{d,l}$ and $\mathbf{B}_{d,l}$ are the discretized versions of the matrices

$$\mathbf{A}_l = -(1/\mu)\,\mathbf{I}_{n_l}, \mathbf{B}_l = (1/\mu)\,\mathbf{I}_{n_l}.$$

Finally, in the last constraint (13b), $P_{\mathbf{min}}$ denotes the minimum power used as a lower bound to avoid solutions implying the shutting-down of some turbines.

The cost function (13a) covers three objectives:

1. Minimizing the tracking error, i.e., $J_1(\mathbf{x}_l(k),\ P^{\mathbf{p}}_{\mathbf{r},l}(k)) \triangleq \left| |P^{\mathbf{p}}_{\mathbf{r},l}(k) - \sum_{i=1}^{n_l} x_{l,i}(k)| \right|_2$, where $P^{\mathbf{p}}_{\mathbf{r},l}$ is the set-point imposed by the CC.
2. Maximizing the available power, i.e., $J_2(\mathbf{u}_l(k)) \triangleq \mathbf{R}\,\mathbf{u}_l(k)_2$, where the elements of the matrix $\mathbf{R}$ are defined as

$$[\mathbf{R}]_{ij} = \begin{cases} (\tau_i + \kappa)^{-\lambda}, & \textbf{if } i = j,\ \lambda = \textbf{max}\left(0, \left(P^{\mathbf{p}}_{\mathbf{av},l} - P^{\mathbf{p}}_{\mathbf{r},l}\right) \Big/ P^{\mathbf{p}}_{\mathbf{av},l}\right), \\ 0, & \textbf{if } i \neq j. \end{cases}$$

Here τ_i is the network resource-feeding index introduced in Section 3, $P^{\mathbf{p}}_{\mathbf{av},l}$ is the total available power in the subset $\mathscr{P}_l$ and $\kappa > 0$ is a small constant to avoid singularity when the turbines are not affected by wakes. When $P^{\mathbf{p}}_{\mathbf{r},l}$ is lower than the total available power, $J_1 = 0$ can be achieved with different power contributions from each turbine. This degree-of-freedom can be used to maximize the available power and thus the power reserve. Inspired by the backward scheme presented in Ref. [28], here a simpler approach is proposed based on penalizing the contributions of the most upstream turbines. The idea consists in reducing the contribution of the upstream turbines to reduce the wind speed deficits faced by the downstream turbine. As the power demand $P^{\mathbf{p}}_{\mathbf{r},l}$ is close to the available power, the backward distribution may not be effective. In order to mitigate this issue, the exponent λ ($0 \leq \lambda \leq 1$), defined as the ratio between the power reserve and the available power, is reduced. Thus, in circumstance of high power demands, all turbines contribute with the same power, whereas, for higher derating operations, the backward distribution is used.

3. Limiting fast variations of the control inputs to smooth the operation and avoid possible damage on the turbine, $J_3(\mathbf{u}_l(k)) \triangleq \| \mathbf{u}_l(k) - \mathbf{u}_l(k-1)\|_2$.

4.3. Central controller (CC)

The aim of the CC is to ensure the entire wind farm delivers the power $P_{\mathbf{dem}}$ required by the TSO. To this end, the CC receives, from each PLC, information about the total generated power $P^{\mathbf{p}}_{\mathbf{w},l}$ and the total available power $P^{\mathbf{p}}_{\mathbf{av},l}$ corresponding to the partition, and then produces a set of power references for each subset $P^{\mathbf{p}}_{\mathbf{r},l}$.

As a consequence of the partitioning procedure, all turbine subsets can be considered uncoupled. Moreover, as only the total power is relevant to this analysis and in order to keep the controller simple, the dynamic response of each partition can be described by a first-order system representing an aggregated wind turbine as follows

$$\dot{P}^{\mathbf{p}}_{\mathbf{w},l} = -\frac{1}{\mu_l}\left(P^{\mathbf{p}}_{\mathbf{w},l} - P^{\mathbf{p}}_{\mathbf{r},l}\right).$$

where μ_l is a time constant that depends on the number of turbines in $\mathscr{P}_l$ and the PLC.

The CC relies on an MPC strategy based on the following optimization problem:

$$\underset{\mathbf{u_p}(k)}{\textbf{minimize}} \sum_{k=1}^{H_{\mathbf{p}}-1} ||\mathbf{Q}\,\mathbf{x_p}(k)||_2 + \|\,\mathbf{S}\,(\mathbf{u_p}(k) - \mathbf{u_p}(k-1))\|_2 \tag{14a}$$

$$\textbf{subject to } \mathbf{x_p}(k+j+1|k) = \mathbf{E}_d \mathbf{x_p}(k+j|k) + \mathbf{F}_d \mathbf{u_p}(k+j|k) + \mathbf{G}_d P_{\mathbf{dem}}(k+j|k), \tag{14b}$$

$$\mathbf{P^p_{min}} \leq \mathbf{u_p}(k+j) \leq \mathbf{P^p_{av}}, \tag{14c}$$

with $k \in \mathbb{N}$, $j \in \{0, \ldots, H_{\mathbf{p}} - 1\}$, and $H_{\mathbf{p}}$ the prediction horizon. As for the PLC, (14b) corresponds to the discrete version of the following approximated dynamic model of the entire wind farm:

$$\dot{\mathbf{x}}_{\mathbf{p}}(t) = \mathbf{E}\,\mathbf{x}_{\mathbf{p}}(t) + \mathbf{F}\,\mathbf{u}_{\mathbf{p}}(t) + \mathbf{G}\,P_{\mathbf{dem}}(t), \tag{15}$$

where

$$x_p = \begin{bmatrix} P^p_{w,1} & \ldots & P^p_{w,m}, & \xi \end{bmatrix}^T, \xi = P_{dem} - \sum_{i=1}^{m} P^p_{w,i}\Big),$$

$$u_p = \begin{bmatrix} P^p_{r,1} & \ldots & P^p_{r,m} \end{bmatrix}^T, E = \begin{bmatrix} -1/\mu_1 & 0 & \ldots & 0 \\ 0 & \ddots & \vdots & \vdots \\ \vdots & & -1/\mu_m & \vdots \\ -1 & \ldots & -1 & 0 \end{bmatrix},$$

$$F = \begin{bmatrix} 1/\mu_1 & 0 & \ldots \\ 0 & \ddots & \vdots \\ \vdots & & 1/\mu_m \\ 0 & \ldots & 0 \end{bmatrix}, G = \begin{bmatrix} 0 \\ \vdots \\ 0 \\ 1 \end{bmatrix}.$$

Constraint (14c) ensures the power references remain within the operating limits given by the minimum power

$$\mathbf{P^p_{min}} = [\, n_1 P_{\mathbf{min}} \quad \ldots \quad n_m P_{\mathbf{min}} \,]^T$$

to avoid shutting-down partitions and the available power defined as

$$\mathbf{P^p_{av}} = \begin{bmatrix} P^{\mathbf{p}}_{\mathbf{av},1} & \ldots & P^{\mathbf{p}}_{\mathbf{av},m} \end{bmatrix}^T,$$

where $P^{\mathbf{p}}_{\mathbf{av},l} = \sum_{i \in \mathscr{P}_l} P_{\mathbf{av},i}$.

In the cost function (14a) is the sum of two objectives, the first is included to minimize the error in the tracking of the power demand. Therefore, the matrix $\mathbf{Q} = \mathbf{diag}(0, \ldots, 0, Q_\xi)$ penalizes only the integral of the tracking error. The second objective is related to the smooth operation and, the matrix $\mathbf{S}$ penalizes the rate of variation of the power references.

5. Case study

The proposed partitioning approach and control strategy were tested for a wind farm of 210 MW rated power with 42 benchmark NREL-5MW wind turbines [29] spaced 630 m (i.e.5 rotor diameters) and placed as shown in Fig. 4. The wind field and wake effect have been simulated for the free-stream wind speed of $v_\infty = 11$ m/s

using SimWindFarm [21], a MATLAB/Simulink toolbox for wind farm simulation and control. The MPC controllers were implemented with YALMIP [30] and CPLEX.

5.1. Wind farm partitioning

As mentioned in Section 3, the proposed partitioning approach depends on the predominant wind speed direction φ and is time-consuming for wind farm layout as the analyzed in this section. Therefore, the partitions were computed offline for the set of angles

$$\mathbf{\Phi} = \{\varphi = (30 \cdot i)^\circ, \quad i = 0, 1, \ldots, 11\}.$$

A justification of this selection can be found in Section 5.2. The partition obtained using the procedure in Section 3 for a wind speed direction of $\varphi = 30^\circ$ is illustrated in Fig. 4. The flow-based distribution graph $\overline{\mathcal{G}} = (\overline{\mathcal{V}}, \overline{\mathcal{E}})$ is obtained by relating each turbine in the information sharing graph $\mathcal{G}$ to an element of the flow based distribution system. The network resource feeding indices $\tau_{\mathbf{i}}$ for each sink $i \in \mathcal{V}_{\mathbf{si}}$ and the respective sources $j \in \mathcal{V}_{\mathbf{so}}$ for the investigated farm layout are given in Table 1.

The appropriate number of subsets in the partition was determined based on two conditions: 1) the maximum sink co-relation index has been set as $\sigma^* = 0.3$, i.e., on each subset the number of sink elements is lower than the 30% of the total amount of sink elements. The first conditions ensures that the number of sinks is almost balanced among the subsets. 2) The minimum resource feeding co-relation index β^* per subset was set at 0.5, i.e., at least half of the source elements feeding the most affected sink in the subset is included in the same subset. These conditions have been defined since they provided the number of subsets that ensures a suitable trade-off between power generation performance and computational burden for solving the proposed optimal control, as it will be presented in the dedicated case study in paragraph Section 5.3. Notice that further conditions may be added to determine the initial number of subsets required for finding the optimal partition. For the chosen parameters, the minimum number of subsets ensuring the desired values of σ^* and β^* is $m = 6$, i.e. $\mathcal{K} = \{1, \ldots, 6\}$. Thus, the maximum resource-feeding index for each subset τ_l^*, with $l \in \mathcal{K}$, along with the corresponding turbine $i \in \mathcal{V}_l$ for which $\tau_i = \tau_l^*$ is: $\tau_1^* = 3$ for $\mathbf{T}_{(42,35)}$, $\tau_2^* = 3$ for $\mathbf{T}_{(27)}$, $\tau_3^* = 2$ for $\mathbf{T}_{(41,42)}$, $\tau_4^* = 2$ for $\mathbf{T}_{38}$, $\tau_5^* = 2$ for $\mathbf{T}_{(13,14)}$ and $\tau_6^* = 3$ for $\mathbf{T}_{(21,28)}$.

The weights in (5) were set as $w_1 = 0.7$, $w_2 = 0.1$ and $w_3 = 0.2$, in order to provide the highest priority at the maximization of the coupling due to the wake effect among turbines in the same subsets. Meanwhile, lower priority is set for the third objective function f_3, to balance the number of turbines at each partition by minimizing the difference of the number of turbines belonging to different partitions. Finally, the lower priority is set for the second objective f_2 since it is only relevant to ensure an optimal solution at partitioning problem when there is no wake interaction among the turbines. It is worthwhile to note that increasing the value of w_3 at the expense of the weight w_1 might yield a different result since the difference among the numbers of turbines in the subset gets close to zero.

5.2. Control design

In order to design the MPC strategies, the time constant in (11) was set to $\mu = 0.125$ s. Notice that this value has been obtained by modeling the wind turbine power input/power output response as a first-order system. For the PLC, the sampling time used to discretize the partition model in (11) was set to 0.05 s, the prediction horizon to $H_{\mathbf{p}} = 3$, and the weights in (13a) to $\gamma_1 = 0.45$, $\gamma_2 = 0.35$ and $\gamma_3 = 0.2$. Thus, total power regulation and maximization of available power have higher priority than control input limitations. For the CC in (14), the sampling time was set to 0.1 s, the prediction horizon at $H_{\mathbf{p}} = 3$, and the weights to $Q_\xi = 0.8$ and $\mathbf{S} = 0.2 \cdot \mathbf{I}_6$ to prioritize the tracking of the power demanded by the grid. The time constants μ_l for each partition $l \in \mathcal{K}$ are given in Table 2. They have been computed by modeling the open-loop power response for a given power input of each partition as a first-order system with time constant μ_i. Notice that such an assumption can be done when the internal variables (individual power, mechanical load, pitch reference, etc.) are not in the controller design [12]. As the number of turbines in each subsets is different, the time constants μ_l needed to approximate the dynamics of each subset are also different.

In order to highlight the effect of redistributing the power contribution of each wind turbine in the partition, in all simulations, for all $t < t_0 = 50$ s the weight on the control input in (13) is selected as $\mathbf{R} = \mathbf{I}_{n_l}$, i.e., equal contribution is required for every turbine, whereas, for all $t \geq t_0$ the contribution are distributed as discussed in Section 4.

5.3. Test 1: power regulation

First, the proposed control strategy was evaluated in the case of a predominant wind speed direction of $\varphi = 30^\circ$ and a power demanded by the TSO of $P_{\mathbf{dem}} = 60$ MW. Hence, the wind farm operates in derated mode, as the total available power simulated in steady-state conditions $P_{\mathbf{av,tot}}$ is almost 60% higher than the power demand. The partitioning in this case results in the following subsets:

$$\begin{aligned}
\mathcal{P}_1 &= \{8,\ 16,\ 17,\ 24,\ 25,\ 33,\ 34,\ 35,\ 42\},\\
\mathcal{P}_2 &= \{1,\ 2,\ 9,\ 10,\ 18,\ 19,\ 26,\ 27\},\\
\mathcal{P}_3 &= \{15,\ 22,\ 23,\ 31,\ 32,\ 39,\ 40,\ 41\},\\
\mathcal{P}_4 &= \{29,\ 30,\ 36,\ 37,\ 38\},\\
\mathcal{P}_5 &= \{5,\ 6,\ 7,\ 13,\ 14\},\\
\mathcal{P}_6 &= \{3,\ 4,\ 11,\ 12,\ 20,\ 21,\ 28\}.
\end{aligned}$$

Fig. 4 illustrates the partitioning and the wake effect.

Fig. 5a shows the total power generated $P_{\mathbf{w,tot}}$ (black line), the set-point $P_{\mathbf{dem}}$ (gray line) and the total available power $P_{\mathbf{av,tot}}$ (blue line). The redistribution of the power contribution starts to affect the available power only after $t = t_0 + t_{\mathbf{w}}$, where $t_{\mathbf{w}} \approx 60$ s is the time the wind takes to travel from one turbine to the next downstream one [31]. Comparing the initial and final values of $P_{\mathbf{av,tot}}$, it can be observed that the power contributions imposed by each PLC are capable of increasing the power reserve with about 2.7% (from 167.5 MW at $t = t_0$ to 172 MW at $t = 600$ s) without affecting the power demand tracking.

Table 1
Sinks, resource feeding indexes and sources in the directed graph $\overline{\mathcal{G}}$ and their connection with the turbines in the information sharing graph $\mathcal{G}$.

$\mathbf{T}_i$ Sink, $i \in \mathcal{V}_{\mathbf{si}}$	τ_i, $i \in \mathcal{V}_{\mathbf{si}}$	$\mathbf{T}_j$ Source, $j \in \mathcal{V}_{\mathbf{so}}$
$\mathbf{T}_{37}$	1	$\mathbf{T}_{29}$
$\mathbf{T}_{38}, \mathbf{T}_{39}, \mathbf{T}_{10}, \mathbf{T}_{13}, \mathbf{T}_{14}$	2	$\mathbf{T}_{(29,30)}, \mathbf{T}_{(22,30)}, \mathbf{T}_{(15,22)}, \mathbf{T}_{(4,5)}, \mathbf{T}_{(6,7)}$
$\mathbf{T}_{41}, \mathbf{T}_{42}, \mathbf{T}_{35}, \mathbf{T}_{27}, \mathbf{T}_{28}, \mathbf{T}_{21}$	3	$\mathbf{T}_{(15,16,22)}, \mathbf{T}_{(8,15,16)}, \mathbf{T}_{(1,8,16)}, \mathbf{T}_{(1,2,8)}, \mathbf{T}_{(1,2,3)}, \mathbf{T}_{(2,3,4)}$

Table 2
Time constants μ_l and the number of turbines in each subset $\mathscr{P}_l$ for different wind speed directions.

Wind speed direction φ	Partitions											
	$\mathscr{P}_1$		$\mathscr{P}_2$		$\mathscr{P}_3$		$\mathscr{P}_4$		$\mathscr{P}_5$		$\mathscr{P}_6$	
	n_1	μ_1 (s)	n_2	μ_2 (s)	n_3	μ_3 (s)	n_4	μ_4 (s)	n_5	μ_5 (s)	n_6	μ_6 (s)
0°	7	0.28	7	0.28	7	0.28	7	0.28	7	0.28	7	0.28
30°	9	0.30	8	0.28	8	0.26	5	0.21	5	0.18	7	0.25
60°	12	0.16	6	0.15	6	0.15	6	0.15	6	0.15	6	0.15
90°	9	0.3	9	0.3	6	0.18	6	0.18	6	0.18	6	0.18

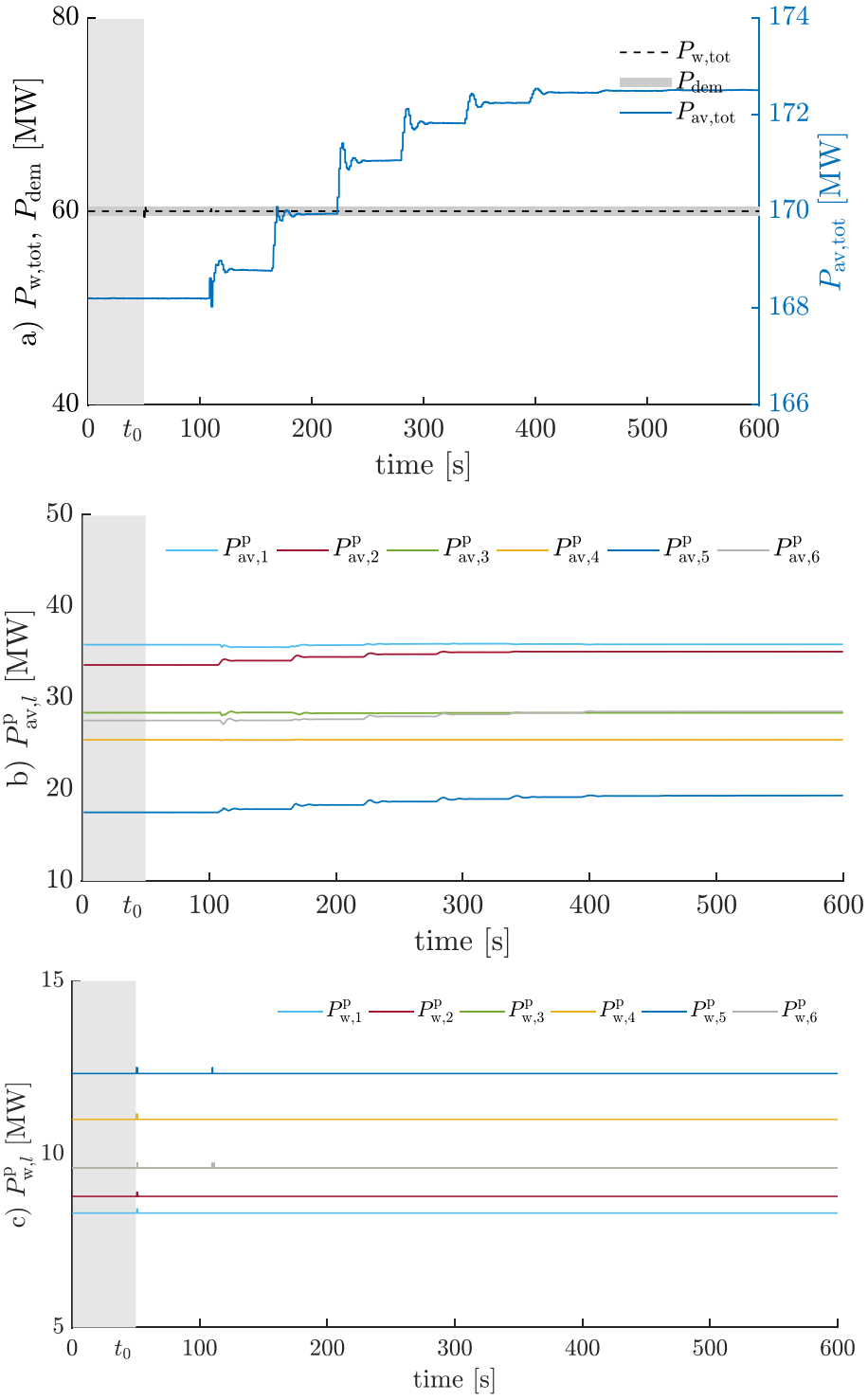

Fig. 5. Test 1: Closed-loop response for $P_{\mathbf{dem}} = 60$ MW, $\varphi = 30°$, and $v_\infty = 11$ m/s. a) Total generated and available power, b) Available power for each partition, c) Generated power for each partition.

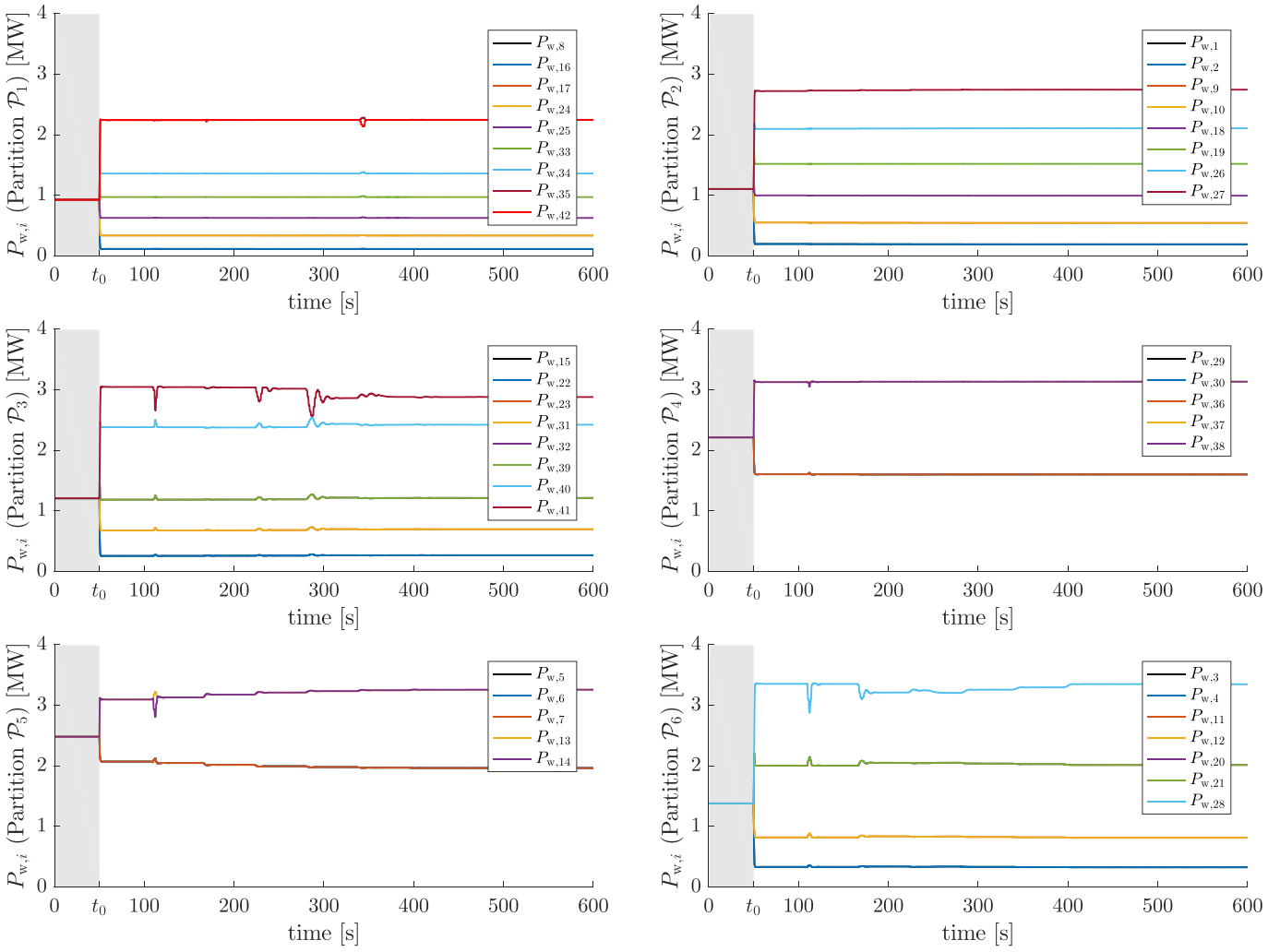

Fig. 6. Test 1: Closed loop response for $P_{\mathbf{dem}} = 60$ MW, $\varphi = 30^\circ$, and $v_\infty = 11$ m/s. Generated power by every turbine in each partition.

Fig. 5b and c shows the available and generated powers, $P^{\mathbf{p}}_{\mathbf{av},l}$ and $P^{\mathbf{p}}_{\mathbf{w},l}$ respectively, for each subset. It can be observed that Subsets $\mathscr{P}_4$ and $\mathscr{P}_5$ make the higher contributions ($P^{\mathbf{p}}_{\mathbf{w},5} = 12.4$ MW, $P^{\mathbf{p}}_{\mathbf{w},4} = 11$ MW), whereas the lowest ones are observed in case of Subsets $\mathscr{P}_1$ and $\mathscr{P}_2$ ($P^{\mathbf{p}}_{\mathbf{w},1} = 8.2$ MW, $P^{\mathbf{p}}_{\mathbf{w},2} = 8.8$ MW). The remaining subsets produce $P^{\mathbf{p}}_{\mathbf{w},3} = P^{\mathbf{p}}_{\mathbf{w},6} = 9.6$ MW. In Fig. 5b, the available power $P^{\mathbf{p}}_{\mathbf{av},l}$ increases in all subsets compared with the initial values, except for Subsets $\mathscr{P}_3$ showing a small reduction (close to 1.5%).

Fig. 6 shows the power generated by each turbine in each partition. It can be observed the backward distribution of the power contribution of each turbine imposed by the PLCs in each partition. The largest contribution is done by the most downstream turbines whereas the most upstream ones tend to reduce the power generation. In this scheme, the power generation of some of the upstream turbines reaches the minimum value $P_{\mathbf{min}}$.

Fig. 7 shows the total available power for different values of power demand: $P_{\mathbf{dem}} = 60$ MW (blue line), 70 MW (red line), 80 MW (yellow line) and 100 MW (purple line). It can be observed that, in cases of high derating operations ($P_{\mathbf{dem}} < 80$ MW), the total available power increases compared to the values obtained with the uniform power contribution scheme ($t < t_0$). In these circumstances, the coefficient λ used in the weight $\mathbf{R}$ in (13a) results to be 0.64 and 0.5, respectively, and the power contribution of each

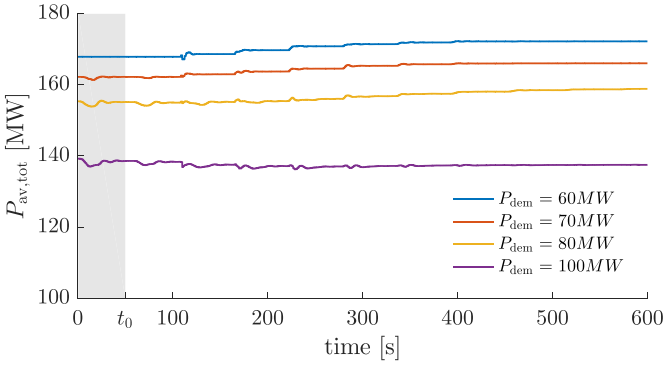

Fig. 7. Test 1: Total available power for several set-points of $P_{\mathbf{dem}}$.

turbine at each subset is determined according to the backward distribution. On the other hand, when the power demand is close to $P_{\mathbf{av,tot}}$, λ is close to zero and the matrices $\mathbf{R}$ tend to $\mathbf{I}_{n_l}$. As a result, the set-points $P_{\mathbf{r},i}$ are similar and every turbine in the partition is required to contribute approximately the same power level. The motivation for using this scheme is due to the fact that when $P_{\mathbf{dem}}$ is high, turbines reach their maximum power limits, especially the most downstream ones, and the backward distribution stops being

effective.

5.4. Test 2: sensitivity to wind speed directions

In this test, the proposed non-centralized control strategy is evaluated when the partitioning does not correspond to the exact predominant wind speed direction. In this test, the proposed non-centralized control strategy is evaluated when the partitioning does not correspond to the exact predominant wind speed direction. As previously mentioned, the subset is computed offline for different sets of directions and selected from a table with an estimated wind speed direction. The aim of this test is to analyze the effect of this approximation on the robustness and performance of the proposed control scheme when there is uncertainty in the

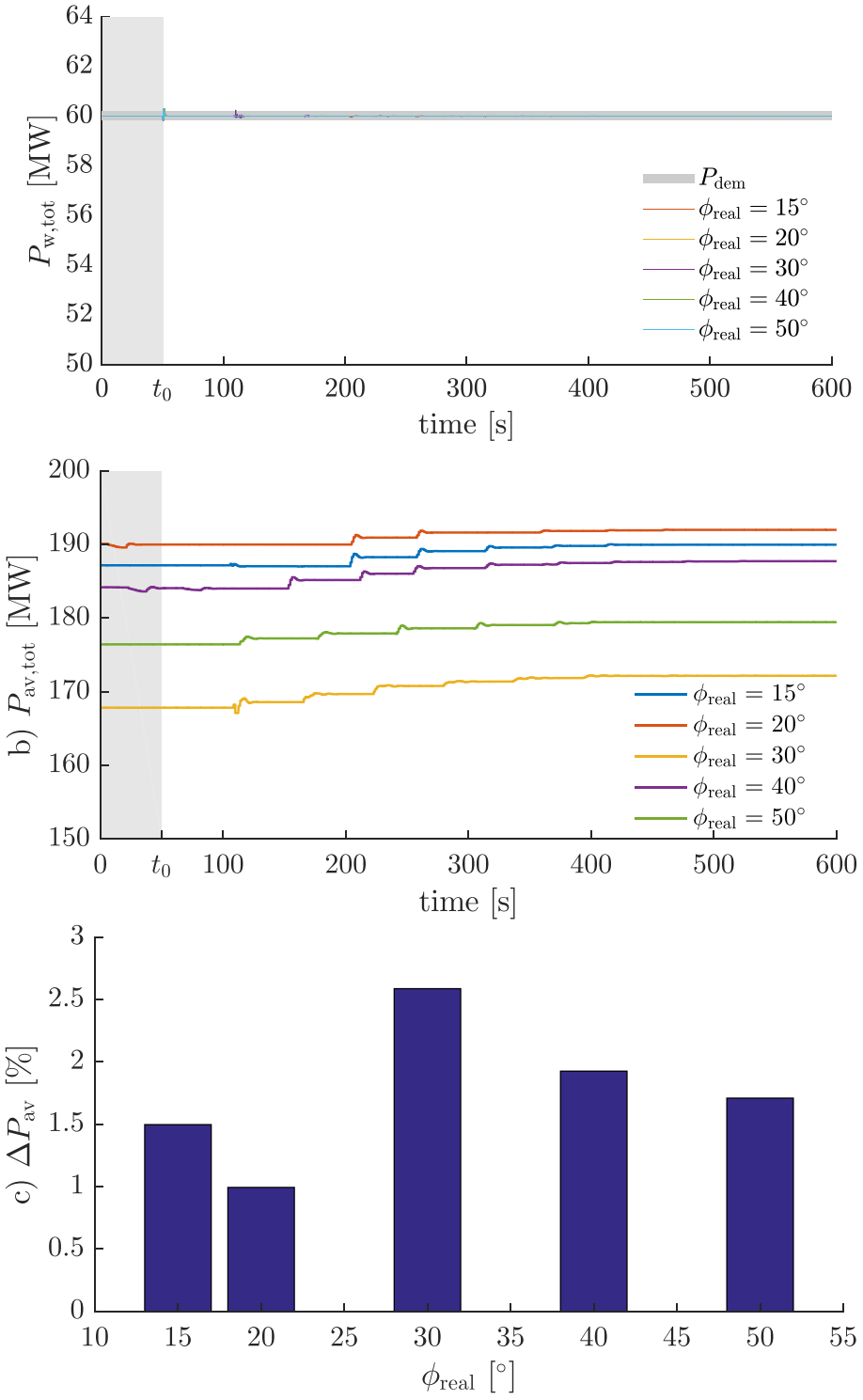

Fig. 8. Test 2: Closed-loop response when the controller is based on a wind speed direction of 30° but the real direction is $\varphi_{\mathbf{real}}$. a) Total generated power, b) Total available power. c) Total available power increment (16).